3-1-1981

Onset of Convection in a Permeable Medium Between Vertical Coaxial Cylinders

Haim H. Bau
University of Pennsylvania, bau@seas.upenn.edu

Kenneth E. Torrance
University of Pennsylvania

Onset of Convection in a Permeable Medium Between Vertical Coaxial Cylinders

Abstract
The onset of natural convection is examined for a fluid-saturated permeable medium contained between vertical coaxial cylinders of inner and outer radii r^*_i and r^*_0. The annular space is of height h^*. The horizontal boundaries are isothermal, with heating from below and cooling from above. Both permeable and impermeable upper boundaries are considered. Critical Rayleigh numbers Ra_c and the preferred convective modes are determined as functons of the geometric ratios h^*/r^*_i and r^*_0/r^*_i. The confining vertical walls of the annular space tend to increase Ra_c above the value for an infinite horizontal layer. The preferred modes are predominantly asymmetric.

Disciplines
Engineering | Mechanical Engineering

Comments
Suggested Citation:
Bau, Haim H. and Kenneth E. Torrance. (1981). *Onset of convection in a permeable medium between vertical coaxial cylinders.* Physics of Fluids. Vol. 24(3).

Onset of convection in a permeable medium between vertical coaxial cylinders

Haim H. Bau and K. E. Torrance

Sibley School of Mechanical and Aerospace Engineering, Cornell University, Ithaca, New York 14853
(Received 24 July 1980; accepted 14 November 1980)

The onset of natural convection is examined for a fluid-saturated permeable medium contained between vertical coaxial cylinders of inner and outer radii r_i^* and r_0^*. The annular space is of height h^*. The horizontal boundaries are isothermal, with heating from below and cooling from above. Both permeable and impermeable upper boundaries are considered. Critical Rayleigh numbers Ra_c and the preferred convective modes are determined as functons of the geometric ratios h^*/r_i^* and r_0^*/r_i^*. The confining vertical walls of the annular space tend to increase Ra_c above the value for an infinite horizontal layer. The preferred modes are predominantly asymmetric.

I. INTRODUCTION

The onset of natural convection in fluid-saturated permeable media heated from below has been examined for infinite layers,[1] rectangular parallelepipeds,[2] and circular cylinders.[3] The present paper considers the annular space between vertical coaxial cylinders. The annular space is confined by horizontal, isothermal boundaries and is heated from below and cooled from above. The vertical walls are adiabatic. The resulting convection in the annulus may assume a wide variety of convective or modal patterns. In this paper, the critical conditions and preferred mode shapes at the onset of convection are determined by using a linear stability analysis.

II. FORMULATION

Consider the vertical, annular cylinder shown in Fig. 1. The inner and outer radii are denoted by r_i^* and r_0^*, respectively. The height is h^*. The vertical walls and the base are impermeable to flow. A fluid-saturated, permeable medium fills the annulus. The upper boundary condition is taken as either impermeable or permeable. The latter is appropriate if a standing liquid overlies the permeable medium. The horizontal boundaries at $z^*=0$ and $z^*=-h^*$ are kept at constant temperatures T_0^* and T_1^*, respectively. The vertical boundaries are adiabatic.

The linearized, steady-state, Darcy–Oberbeck–Boussinesq equations[4] in nondimensional form are

$$\nabla\cdot\mathbf{q}=0\,,\quad \nabla^2 w=\mathrm{Ra}^{1/2}\nabla_1^2\theta\,,\quad -\nabla^2\theta=\mathrm{Ra}^{1/2}w\,, \tag{1}$$

where $\mathbf{q}$ is the velocity vector, w is the vertical velocity, θ is the temperature, and $\nabla_1^2=\nabla^2-\partial^2/\partial z^2$. The dependent variables represent small disturbance quantities relative to a rest state with a linear conduction temperature profile. The Rayleigh number which appears is defined by

$$\mathrm{Ra}=\frac{gK\beta_f(T_1^*-T_0^*)h^*}{\nu_f(\lambda_m/\rho_f c_{pf})}\,, \tag{2}$$

where g is the gravitational acceleration, K is the permeability, β_f is the volume thermal expansion coefficient of the fluid, ν_f is the kinematic viscosity of the fluid, λ_m is the thermal conductivity of the saturated medium, ρ_f is the fluid density, and c_{pf} is the fluid specific heat. Reference quantities for the nondimensionalization are h^* for length, $(T_1^*-T_0^*)$ for temperature, and $\mathrm{Ra}^{-1/2}\lambda_m/\rho_f c_{pf}h^*$ for velocity. Variables with asterisks are dimensional; the same variables without asterisks are nondimensional.

The boundary conditions associated with (1) which are applicable to the annular cylinder are

$$v=\theta_r=0\,,\quad \text{at } r=r_i^*/h^* \text{ and } r=r_0^*/h^*\,,$$
$$w=\theta=0\,,\quad \text{at } z=-1\,,$$
$$\theta=0\,,\quad \text{at } z=0\,, \tag{3}$$

and, at $z=0$,

$$w=0 \text{ when impermeable}\,,$$
$$w_z=0 \text{ when permeable}\,.$$

The last boundary condition of $w_z=0$ corresponds to a constant pressure condition at the permeable upper boundary. Note that the subscripts r, ϕ, and z denote differentiation with respect to the radial, azimuthal, and axial coordinates. At the adiabatic vertical walls, the boundary condition of $v=0$ on the radial velocity is equivalent to $w_r=0$.

We note that the onset of convection is characterized by the monotonic growth of disturbances in time; this is the principle of exchange of stabilities.[5] Thus, the critical state is time-independent and the steady-state equations (1) are applicable.

III. SOLUTION

The governing equations and boundary conditions may be reduced to

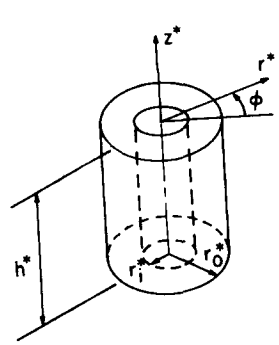

FIG. 1. Sketch of geometry and coordinate system. A permeable medium fills the vertical, annular cylinder.

 0031-9171/81/030382-04$00.90

$$\nabla^4\theta + \mathrm{Ra}\nabla_1^2\theta = 0\,,$$

$$\theta_r = \nabla^2\theta_z = 0 \quad \text{at } r = r_i,\ r_0\,,$$

$$\theta = \nabla^2\theta = 0 \quad \text{at } z = -1\,,$$

$$\theta = 0 \quad \text{at } z = 0\,, \tag{4}$$

and

$$\nabla^2\theta = 0 \quad \text{at } z = 0 \text{ when impermeable}\,,$$

$$\nabla^2\theta_z = 0 \quad \text{at } z = 0 \text{ when permeable}\,.$$

Separation of variables leads to

$$\theta = g(z)\left(\frac{J_m(\kappa r)}{J_m'(\kappa r_i)} - \frac{Y_m(\kappa r)}{Y_m'(\kappa r_i)}\right)\cos(m\phi)\,, \tag{5}$$

where m is an integer, J_m and Y_m are Bessel functions of the first and second kinds, respectively, and the primes denote differentiation with respect to r. After applying the radial boundary conditions, the parameters κ are found from

$$J_m'(\kappa r_i)Y_m'(\kappa r_0) - J_m'(\kappa r_0)Y_m'(\kappa r_i) = 0\,, \tag{6}$$

which admits an infinite set of real zeros for fixed values of r_i and r_0. We denote this set by κ_{mp}, where p is an integer. The first twelve zeros have been determined and are tabulated in ascending order elsewhere.[6] For tabulation purposes, it was convenient to tabulate the product $\kappa_{mp}r_i$. In this form, the roots of (6) are a function only of the radius ratio $l \equiv r_0/r_i = r_0^*/r_i^*$.

The linear stability eigenvalue problem is expressed in terms of $g(z)$ by

$$(D^2 - \kappa^2)^2 g - \kappa^2\,\mathrm{Ra}\,g = 0\,, \tag{7}$$

where $D = d/dz$.

For the vertical annulus with an impermeable top, the appropriate boundary conditions for (7) are

$$g = (D^2 - \kappa^2)g = 0 \quad \text{at } z = 0,\ -1 \tag{8}$$

and the resulting solution for g is

$$g = A\sin[n\pi(z+1)]\,, \tag{9}$$

where A is the disturbance amplitude and n is an integer. The spatial structure of the disturbance solution is found by substituting (9) into (5). The associated Rayleigh number is found by substituting (9) into (7), obtaining

$$\mathrm{Ra} = \left(\frac{n^2\pi^2}{\kappa_{mp}} + \kappa_{mp}\right)^2. \tag{10}$$

For the case of a permeable top the appropriate boundary conditions for (7) are

$$g = D(D^2 - \kappa^2)g = 0\,, \quad \text{at } z = 0\,,$$
$$g = (D^2 - \kappa^2)g = 0\,, \quad \text{at } z = -1\,. \tag{11}$$

The resulting solution for g is

$$g = A\left(\frac{\sin[\eta(z+1)]}{\sin\eta} - \frac{\sinh[\xi(z+1)]}{\sinh\xi}\right), \tag{12}$$

$$\eta^2 = \kappa(\mathrm{Ra}^{1/2} - \kappa), \quad \xi^2 = \kappa(\mathrm{Ra}^{1/2} + \kappa)\,.$$

Substitution of (12) into (5) gives the spatial form of the disturbance solution. Substitution into (7) yields a characteristic equation for Ra:

$$\xi\coth\xi + \eta\cot\eta = 0\,. \tag{13}$$

The zeroes of this expression are denoted by the integer n; there are an infinite number of such zeroes for each value of κ_{mp}. Clearly, the zeroes are bounded by

$$(n-1)^2\frac{\pi^2}{4\kappa_{mp}^2} + \kappa_{mp} < \mathrm{Ra}^{1/2} < \frac{n^2\pi^2}{\kappa_{mp}} + \kappa_{mp}\,. \tag{14}$$

We note in passing that Eq. (13) also describes conditions at the onset of convection in a vertical, annular cylinder with an isothermal top and a uniform-heat-flux bottom, both of which are impermeable.[7] Consequently, results from the present study for the critical Rayleigh numbers and preferred convective modes for a permeable-top cylinder also apply, as appropriate, to an annular cylinder with a uniform heat flux at the bottom.

For a given geometry, characterized by the nondimensional radii r_i and r_0, Rayleigh numbers are found by evaluating (10) and (13) for each convective mode in the (m,n,p) integer space. The minimum Rayleigh number from this search yields the critical Rayleigh number, defined by

$$\mathrm{Ra}_c = \min_{m,n,p} \mathrm{Ra}\,, \tag{15}$$

and the preferred convective pattern at the onset of motion. We note from (10) and (14) that the minimum Ra always occurs for the $n = 1$ vertical mode. Thus, the search is over the (m,p) modes, which represent the horizontal planform modes.

IV. RESULTS AND DISCUSSION

A. The critical Rayleigh number

Critical Rayleigh numbers are shown in Fig. 2 for annular cylinders with permeable and impermeable upper boundaries. The radius ratio $l = r_0^*/r_i^*$ is held fixed ($l = 1.1$), while the radius/height ratio $r_i = r_i^*/h^*$ is the abscissa.

Clearly, critical Rayleigh numbers in Fig. 2 for a permeable upper boundary are lower than for an impermeable upper boundary. The destabilizing effect of a permeable upper boundary has been previously noted for an infinite layer[1,7] and could be anticipated for the annular cylinder by comparing Eqs. (14) and (10).

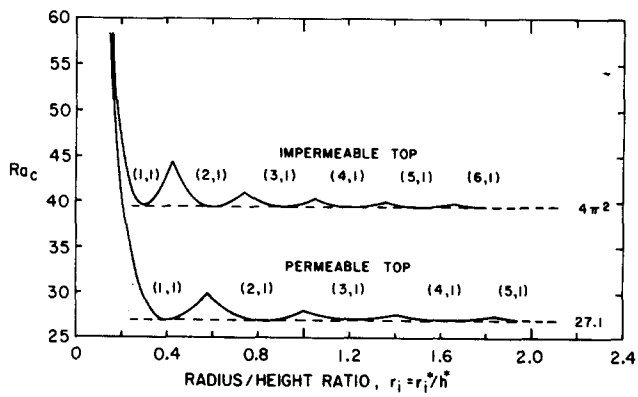

FIG. 2. Critical Rayleigh numbers (Ra_c) and the preferred convective modes (m,p) at the onset of convection in annular cylinders with permeable and impermeable upper boundaries. The radius ratio is $l = r_0^*/r_i^* = 1.1$. Dashed lines indicate results for an infinite horizontal layer.

For large values of r_i, Ra_c asymptotically approaches the values for an infinite layer of $4\pi^2$ (impermeable top) and 27.1 (permeable top). It is readily shown that these are also the lower bounds for Ra_c, and are achieved at discrete values of r_i. The stabilizing effect of the vertical walls is especially significant for low radius/height ratios ($r_i \to 0$). The resulting increase in Ra_c is shown in Fig. 2. As the radius/height ratio decreases (the cylinder becomes taller), the effect of the top boundary condition decreases, and results for the permeable and impermeable cases coincide.

B. The preferred convective modes

In Fig. 2, the preferred convective modes are indicated by the integer values (m,p) along each curve. The planform structure in the (r, ϕ) plane may be inferred from Eq. (5). Results similar to those in Fig. 2 have been obtained for radius ratios up to $l = r_0^*/r_i^* = 2.5$. The convective mode selection is shown in Figs. 3 and 4 for the cases of impermeable and permeable upper boundaries, respectively. Discrete zones are apparent in which particular convective modes (m,p) are preferred. Modes corresponding to $m = 0$ are axisymmetric, while those corresponding to $m \neq 0$ are nonaxisymmetric. Hence, the preferred modes are predominantly asymmetric.

The preferred mode shapes in Figs. 3 and 4 are generally similar. However, for the case of a permeable upper boundary, streamlines do not close inside the porous medium. The effective height of the convective motion is larger than the geometric height. Consequently, transitions from one mode to another occur at larger radius/height ratios for a permeable upper boundary than for an impermeable upper boundary.

C. The convective structure

Consider now the three-dimensional structure of the convective modes. Streamlines for various modes are sketched in Fig. 5. Solid streamlines correspond to an impermeable upper boundary; the heavy dashed lines illustrate the change in the streamlines due to a permeable upper boundary.

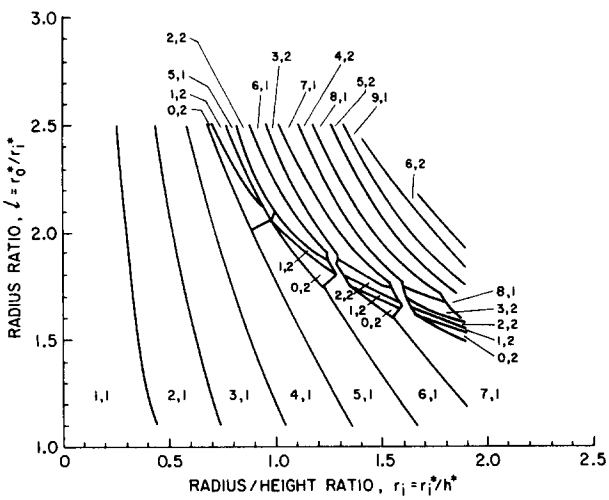

FIG. 3. Map of the preferred convective modes (m,p) in a vertical, annular cylinder with an impermeable top. The governing geometric parameters appear on the axes.

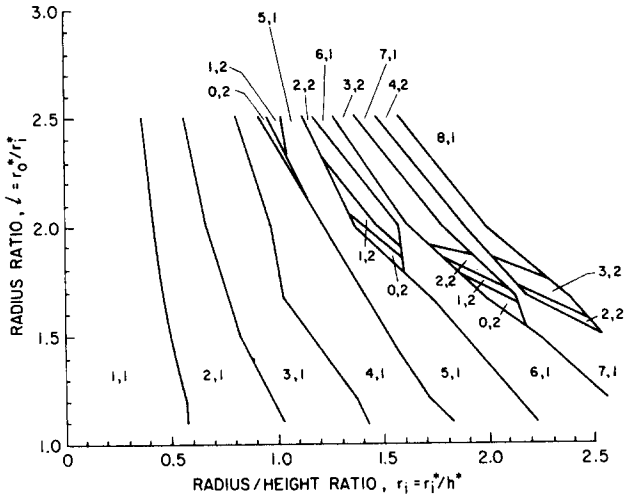

FIG. 4. Map of the preferred convective modes (m,p) in a vertical, annular cylinder with a permeable top. The governing geometric parameters appear on the axes.

The $(m,p) = (1,1)$ mode appears in Fig. 5(a). This mode has a vertical component of velocity which is proportional to $\cos\phi$. This corresponds to, say, ascending flow in the range $\pi/2 < \phi < 3\pi/2$ and descending flow in the range $-\pi/2 < \phi < \pi/2$. The vertical velocity varies only slightly in magnitude across the radius of the annulus (as shown in the left sketch). Streamlines for the flow are thus parallel lines in a radial cross section of the cylinder of height h^* and width $r_0^* - r_i^*$. On the other hand, in the unwrapped circum-

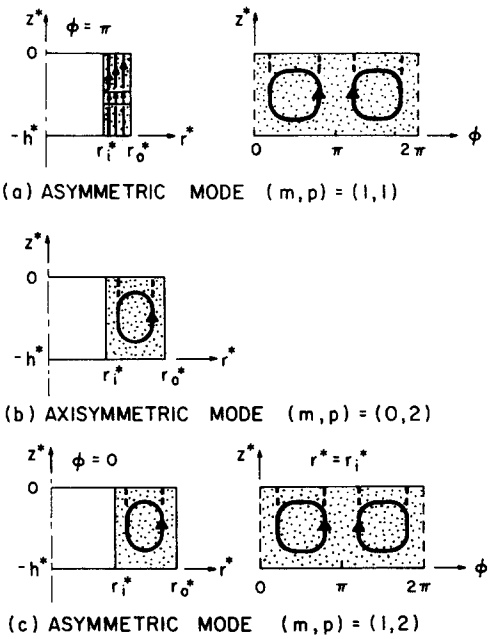

FIG. 5. Structure of three convective modes. Radial cross sections are shown in the left column; the unwrapped circumferential plane is shown in the right column. Solid streamlines correspond to an annular cylinder with an impermeable upper boundary. Heavy dashed streamlines illustrate the effect of a permeable upper boundary.

ferential plane of height h^* and width 2π (or $2\pi r_i^*$), two counter-rotating vortices appear. These vortices penetrate, or do not penetrate, the upper boundary depending upon whether the upper boundary is permeable, or impermeable. The convective modes $(m,p)=(2,1)$, $(3,1)$, $(4,1)$,... correspond, respectively, to 4, 6, 8,... vortices in the unwrapped circumferential plane. All of these modes are clearly nonaxisymmetric; their spatial structure is very similar to the preferred convective modes in a thin, rectangular box[3] of height h^*, width $2\pi r_i^*$, and thickness $r_0^* - r_i^*$. For such a box (in the limit of small thickness), the resulting motion consists of two-dimensional rolls with axes parallel to the thin dimension.

Axisymmetric modes occur only in small, discrete regions in Figs. 3 and 4. Indeed, the only axisymmetric mode which appears is the $(m,p)=(0,2)$ mode. For example, this is the preferred mode for an annular cylinder with an impermeable top (Fig. 3) of geometry $r_i=0.85$ and $l=2.2$. The associated flow pattern is shown in Fig. 5(b). A single toroidal roll is apparent in the radial cross section. The flow is two-dimensional since the azimuthal velocity is zero everywhere. The direction of rotation of the toroidal vortex is arbitrary, but is shown ascending in the interval $1.65\,r_i^* < r^* \leq 2.2\,r_i^*$, and descending in the interval $r_i^* \leq r^* < 1.65\,r_i^*$.

Higher modes result in complex, three-dimensional structures. The simplest of the complex modes is the $(m,p)=(1,2)$ mode sketched in Fig. 5(c). The flow consists of a single toroidal roll in the radial cross section and a pair of vortices in the unwrapped circumferential plane. The left sketch applies for $\phi=0$; the right sketch for $r^*=r_i^*$. The combined flow is a pair of spiralling half-toroids. The half-toroids are of azimuthal span π and are mirror-symmetric about the plane $\phi=0,\ \pi$.

In general, a mode (m,p) consists of $2m$ vortices in the unwrapped circumferential plane and $(p-1)$ toroidal rolls.

D. The limiting case of a very tall cylinder

As mentioned earlier, the stabilizing effect of the vertical walls is especially significant for small values of the radius/height ratio $r_i=r_i^*/h^*$; that is, for tall cylinders. In this regime, it is convenient to redefine the Rayleigh number as

$$\mathrm{Ra}'=\frac{gK\beta_f(-\partial T^*/\partial z^*)(r_0^*-r_i^*)^2}{\nu_f(\lambda_m/\rho_f c_{pf})}, \tag{16}$$

where $-\partial T^*/\partial z^*$ is the vertical temperature gradient. Note that the cylinder height h^* does not appear in Ra'.

As is apparent from Figs. 3 and 4, the mode $(m,p)=(1,1)$ is the preferred convective structure for tall cylinders filled with a permeable medium. This mode is also the preferred mode for a tall annulus filled with a viscous fluid.[8]

In the limit of small radius/height ratios as $r_i \to 0$, (16) and (10) may be combined to obtain an expression for the critical Rayleigh number

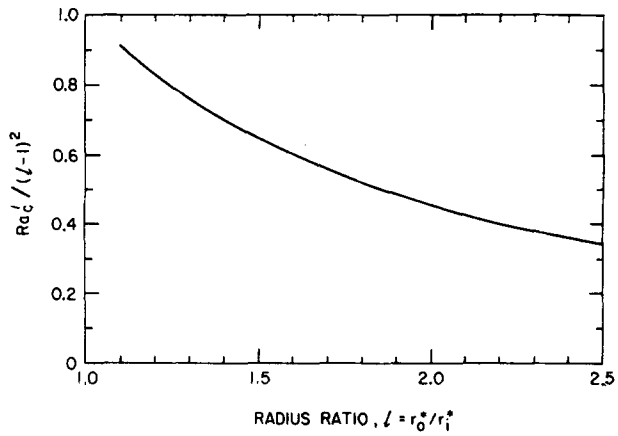

FIG. 6. The critical Rayleigh number for tall annular cylinders. Ra' is defined by (16).

$$\mathrm{Ra}_c'=\kappa_{1,1}^2 r_i^2 (l-1)^2. \tag{17}$$

This result holds for annular cylinders with permeable or impermeable upper boundaries. Since the product $\kappa_{1,1}r_i$ depends only on the radius ratio $l=r_0^*/r_i^*$, Ra_c' is a function only of l. The ratio $\mathrm{Ra}_c'/(l-1)^2$ is shown in Fig. 6 with l as the abscissa. The existence of a common asymptote (as $r_i \to 0$) for both permeable and impermeable upper boundaries is consistent with the results previously shown in Fig. 2, and confirms the decreasing importance of the upper boundary condition as the cylinder becomes taller.

V. CONCLUSIONS

For a vertical, annular cylinder of finite height filled with a permeable medium and heated from below, the preferred convective modes at the onset of convection are predominantly asymmetric. Critical Rayleigh numbers are bounded from below by results for an infinite horizontal layer, and increase sharply as either the radius ratio of the annulus or the radius/height ratio of the cylinder is reduced. When the upper boundary of the annulus is permeable, the critical Rayleigh number is reduced relative to an impermeable upper boundary.

ACKNOWLEDGMENT

This work was supported by the National Science Foundation under Grant ENG-7823542.

[1] E. R. Lapwood, Proc. Cambridge Philos. Soc. **44**, 508 (1948).
[2] J. L. Beck, Phys. Fluids **15**, 1377 (1972).
[3] A. Zebib, Phys. Fluids **21**, 699 (1978).
[4] D. D. Joseph, *Stability of Fluid Motions* (Springer-Verlag, Berlin, 1976), Chap. 10.
[5] S. Chandrasekhar, *Hydrodynamic and Hydromagnetic Stability* (Oxford, London, 1961), Chap. 2.
[6] H. H. Bau, Ph.D. thesis, Cornell University (1980), pp. 109 and 246.
[7] R. J. Ribando and K. E. Torrance, J. Heat Transfer **98**, 42 (1976).
[8] G. Z. Gershuni and E. M. Zhukhoritskii, *Convective Stability of Incompressible Fluids* (Israel Program for Scientific Translations, Jerusalem, 1976), p. 76.